Animal Study

Electroacupuncture Alleviates Thalamic Pain in Rats by Suppressing ADCY1 Protein Upregulation

Bao-Feng Ma, MD[1-3], John P. Williams, MD[4], Jian-Feng Zhang, MD[2,5], Ruo-Guo Wang, MD[1,2], Jian Guo, MD[2], and Jian-Xiong An, MD, PhD[1,2,4,5]

From: [1]School of Anesthesiology, Weifang Medical University & Department of Anesthesiology, Pain & Sleep Medicine, Affiliated Hospital of Weifang Medical University, Shandong, China; [2]Department of Anesthesiology, Pain & Sleep Medicine, Aviation General Hospital of China Medical University & Beijing Institute of Translational Medicine, Chinese Academy of Sciences, Beijing, China; [3]Department of Anesthesiology, The Third Affiliated Hospital of Jinzhou Medical University, Liaoning, China; [4]Department of Anesthesiology, University of Pittsburgh School of Medicine, Pittsburgh, PA, USA; [5]Savaid Medical School, University of Chinese Academy of Sciences, Beijing, China

Address Correspondence: Jian-Xiong An, MD, PhD School of Anesthesiology, Weifang Medical University & Department of Anesthesiology, Pain & Sleep Medicine, Affiliated Hospital of Weifang Medical University, Baotong West St. #7166, Weifang, Shandong, 261053, China E-mail: anjianxiong@yeah.net

Disclaimer: This research was funded by the National Natural Science Foundation of China (grant number 82072086).

Conflict of interest: Each author certifies that he or she, or a member of his or her immediate family, has no commercial association (i.e., consultancies, stock ownership, equity interest, patent/licensing arrangements, etc.) that might pose a conflict of interest in connection with the submitted manuscript.

Manuscript received: 12-11-2021
Revised manuscript received: 12-16-2021
Accepted for publication: 01-25-2022

Free full manuscript: www.painphysicianjournal.com

Background: Thalamic pain (TP), also known as central post-stroke pain, is a chronic neuropathic pain syndrome that follows a stroke and is a severe pain that is usually intractable. No universally applicable and effective therapies have been proposed. Emerging studies have reported that electroacupuncture (EA) can potentially be used as an effective therapy for the treatment of neuropathic pain. However, whether EA influences TP and if so, by what potential mechanism, remains poorly understood.

Objective: The aim of this study was to detect the efficacy of EA and explore possible mechanisms for treating TP.

Study design: Controlled animal study.

Setting: The laboratory at the Aviation General Hospital of China Medical University and Beijing Institute of Translational Medicine.

Methods: Male Sprague Dawley rats were randomly divided into 3 groups (n = 15 / group): sham-operated (SH) group, thalamic pain model (TP) group, EA treatment (EA) group. After the TP rat model was successfully established, EA was used for intervention. During the experiment, the mechanical pain thresholds of rats were detected among the groups. The right thalamus of the rats was extracted on postoperative day 28 for RNA-sequencing (RNA-Seq) analysis to find the changes in gene expression in different groups of rats. The key genes were screened using reverse transcription-polymerase chain reaction (RT-PCR) detection and subsequently identified with western blotting and immunofluorescence.

Results: The mechanical withdrawal threshold (MWT) value of the right facial skin in the TP group and the EA group decreased significantly on the 3rd day after surgery, compared to the SH group ($P < 0.01$). From 7 to 28 days, the MWT value increased continually in the EA group; however, there was no significant change in the TP group. The results of RNA-seq showed that compared to the TP group, 377 genes changed in the EA group. Moreover, ADCY1 expression increased significantly in the TP group as compared to the SH group, while EA treatment reversed the expression of ADCY1.

Limitations: In addition to ADCY1, the mechanism(s) of other signaling pathways in TP need to be explored in future research.

Conclusions: EA treatment may promote the recovery of TP model rat by regulating ADCY1 expression.

Key words: Thalamic pain, neuropathic pain, cobra venom, electroacupuncture, RNA-sequencing analysis, Gene Ontology, Kyoto Encyclopedia of Genes and Genomes, ADCY1

Institutional Review Board (IRB) number: HK2021-06

Pain Physician 2022: 25:E629-E640

Thalamic pain (TP), also known as central post-stroke pain (CPSP), is a severe, continuous or intermittent pain corresponding to the lesion site after cerebrovascular accident (ischemia or hemorrhage) or brain injury, and may be accompanied by sensory abnormalities that can be described generally as chronic neuropathic pain (1). TP syndrome was first systematically described by Dejerine and Roussy in 1906 as spontaneous pain following a thalamic stroke (2). Due to the absence of a clear definition or widely accepted diagnostic criteria, the incidence of TP varies from 8% to 55% of stroke patients (3). The mechanism underlying TP is still poorly understood, but central disinhibition, central sensitization, functional changes in the spinothalamic tract, and thalamic lesions have all been suggested as possible etiologies (4,5). Several pharmacological and nonpharmacological treatments have been suggested, such as antidepressants, anticonvulsants, surgical operations, and cognitive-behavioral therapy; however, these treatment modalities are not widely accepted because of non-negligible side effects and limited therapeutic efficacy (6). Thus, an in-depth understanding of the pathogenesis of TP is required before developing an effective approach for treatment and future research.

Electroacupuncture (EA) is an analgesic method in which fine needles are inserted into an individual at discrete points, and then electrical stimulation is added to those needles with the goal of relieving chronic pain (7). In the last few decades, prior studies have confirmed an analgesic effect of EA stimulation in animals with chronic neuropathic pain (8-10). An et al established a new rat model of TP and found that EA treatment was effective for this kind of pain (11). However, key regulators and specific pathways of EA in the inhibition of TP remain unclear.

In the present study, we used RNA-Sequencing analysis (RNA-Seq) to analyze differences in gene expression, molecular networks, and signaling pathways in ipsilateral thalamic tissues of TP model rats in the presence and absence of EA treatment. These findings might supply further insights and directions for identifying new and effective therapeutic options for TP as well as other types of neuropathic pain.

Methods

Animals

The protocol for this research complied with the guidelines by Institutional Animal Care and Use Committee (IACUC). In this study, 45 Sprague Dawley rats (healthy, adult males) weighing 200-220 g were provided by Charles River Laboratory Animal Co., Ltd. (Beijing, China). They were habituated with 5 animals per cage with food and water freely and housed at a temperature of 22°C-24°C with 40% to 60% humidity and 12 hours on, 12 hours off light/dark cycles. Rats were randomly divided into 3 equal groups (15 rats per group): sham-operated group (SH group), TP model group (TP group), TP model with EA treatment group (EA group). Every attempt was made to minimize the number of animals used and the suffering of the animals.

Establishment of the Experimental Model

We anesthetized the rats using 1% sodium pentobarbital (40 mg/ kg body weight, intraperitoneal [i.p.]; AMRESCO, USA) and placed them in a stereotaxic frame during surgical procedures. Under aseptic conditions, 1μL volume mixture of sterile saline and lyophilized cobra venom (CV, 1 μg /μL , Venom Research Institute of Guangxi Medical University) was injected into the right ventral posterolateral (VPL) thalamic nucleus (bregma -3 mm anterior-posterior; 3 mm lateral to the midline, and 6 mm ventral to the surface of the skull) using a microsyringe pump at 0.1μL/min. The TP and EA group rats were treated with the above methods, while the SH group was injected with an equal volume of the sterile saline vehicle only. After each injection, the syringe remained in position for an additional 10 minutes before it was slowly withdrawn.

EA Stimulation

The procedure for EA treatment was induced as previously described (11). The EA stimulation was applied to the EA group rats every other day from the 7th day to the 28th day after modeling. Two stainless-steel acupuncture needles, 0.25 mm in diameter, were inserted into the right forelimb, one in the Quchi acupoint (LI11) and the other in the Shousanli acupoint (LI10). Then the 2 needles were connected to a Han's acupuncture point nerve stimulator (HANS-200A, Suzhou, Jiangsu, China). The parameters of EA were set as follows: alternating strings of dense-sparse frequencies (2 and 100 Hz shifting automatically, frequency sweeping; pulse width of 0.6 ms at 2 Hz and 0.1 ms at 100 Hz, each lasting for 3 s), intensities ranging from 1.0 to 2.0 mA. The total procedure time was 30 minutes. EA treatment was performed at the same time every day.

Measuring Pain Threshold

The sensitivity to mechanical stimuli was examined as described in a previous study (12). The mechanical withdrawal thresholds (MWTs) of the rats' 4 paws and bilateral faces were measured before creating the model, and again on the 3rd, 7th, 14th, 21st, and 28th day after surgery. The rats were placed individually in wire mesh-bottom cages (30 × 20 × 15 cm) for 15 minutes before assessment. The von Frey hairs (Stoelting Co, Thermo, Gilroy, CA, USA) were applied with different bending forces (0.4, 0.6, 1, 2, 4, 6, 8, 10, and 15 g) to the 6 areas mentioned above. An abrupt withdrawal of the paw, licking, or turning of the head away to avoid stimulation were considered positive responses. The hair corresponded to a force of 4 g was applied first. If the animal's reaction was positive, a weaker one was chosen. In the case of no responses, a stronger stimulus was followed. The interval between each stimulation occurred within 2 minutes. This detection method was carried out at the same time every day. The flow diagram of this experiment is shown in Fig. 1.

RNA Extraction and RNA-Seq Library Establishment

On day 28, 3 randomly-selected rats of each group were deeply anesthetized as described above and perfused transcardially with 250 mL 0.9% NaCl (4°C). The right thalamic tissues were extracted after the perfusion and immediately stored at -80°C for later assessment. Total RNA was isolated and extracted from 3 groups by using Trizol reagent (Invitrogen, Carlsbad, USA). The concentration and purity of the tissues were detected by the Nanodrop spectrophotometer (NanoDrop Products, CA, USA), and their size range and quality were verified on the Agilent 2100 Bioanalyzer (Agilent Technologies, Palo Alto, CA). For sample preparations, a total amount of 2 μ g RNA per sample was used as input material. In brief, we purified mRNA molecule using oligo (dT)-attached magnetic beads from total RNA. First strand cDNA was synthesized, and second strand cDNA synthesis was subsequently performed. The final library size was about 350 base pairs by Qubit-HS quantification. The libraries were sequenced to generate 150 paired-end reads on an Illumina NovaSeq platform.

Pathway Analysis

The functions of genes were described and classified through Gene Ontology (GO) terms. GO enrichment analysis of gene concentration was performed using goatools software and Fisher's exact test. When the corrected *P* value (FDR) < 0.05, the GO function was considered to be significantly rich. Kyoto Encyclopedia of Genes and Genomes (KEGG) is a knowledge base that can systematically analyze gene functions, which closely links genomic information with high order functional information. KEGG pathway was used as the unit of enrichment analysis. The FDR (q-value) of the *P* value and the *P* value corresponding to each pathway were calculated through statistical tests. The way to determine the differentially expressed genes significantly enriched compared with the genome-wide background was to use the corrected *P* value (0.05) as the threshold.

RT-PCR Analysis

The right thalamic tissues were collected and ground into a powder in dry ice. Total RNA was extracted from thalamic tissue with Trizol (G3013, Servicebio, Wuhan, China) and reverse transcribed to cDNA using a reverse transcriptase kit (G3330, Servicebio, Wuhan, China) and oligo (dT) primers (G3205, Servicebio, Wu-

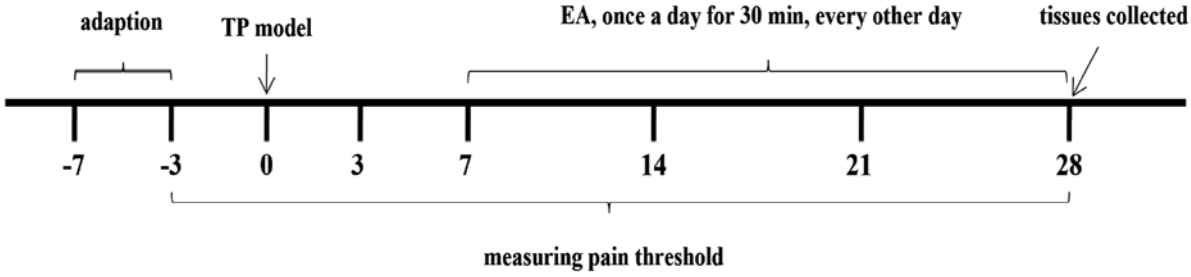

Fig. 1. *Follow chart of study design. All rats adapted to the environment from 7 days before operation. MWTs were measured on preoperative day 3 and day 3, 7, 14, 21 and 28 after surgery. Rats were sacrificed after MWT measurement on day 28 for RNA-Seq. Rats received EA therapy, 2/100 Hz from day 7 to day 28 after surgery and once every other day until the end of this experiment.*

han, China). The primer sequences for PCR were as follows:

ADCY1 forward 5′-GTCATGGAGGCTGCTGGCTTA-3′; reverse 5′-GATGGGATGGCACAATAAAGAAG-3′;

GAPDH forward 5′-CTGGAGAAACCTGCCAAGTATG-3′; reverse 5′-GGTGGAAGAATGGGAGTTGCT-3′. The reverse transcribed products were amplified. The reaction conditions were as follows: 10 minutes at 95°C, followed by 40 cycles of 15 seconds at 95°C, and 30 seconds at 60°C. Then a melting curve program was generated from 65°C to 90°C at a heating rate of 0.1°C per second. Quantitative RT-PCR data were normalized with GAPDH mRNA levels. Relative mRNA levels were expressed as 2-ΔΔCt values.

Western Blotting Analysis

Animals in the 3 groups were anesthetized with sodium pentobarbital after termination of the behavioral test. The right thalamic tissues were isolated on an ice plate rapidly and then washed with Tris-buffered saline. The proteins were obtained using a cell protein extraction kit with protease and phosphatase inhibitors (Servicebio, Wuhan, China) and incubated for 10 minutes at 4°C. Samples (30 μg proteins) were fractionated onto a 10% sodium dodecyl sulfate polyacrylamide gel for about 90 minutes at 80/120 V and then electrotransferred onto polyvinylidene difluoride (PVDF) membranes for 100 minutes at 250 mA. The membranes were blocked in Tris-buffered saline containing 0.05% Tween (TBST) with 5% defatted dry milk for 120 minutes at room temperature. Subsequently they were immuno-labelled with primary antibodies of rabbit anti-ADCY1 (1:1,000; Solarbio, Beijing, China) and rabbit β-actin (1:2,000; Solarbio, Beijing, China) overnight at 4°C. Thereafter the membranes were washed with TBST for 3 times, once for 10 minutes and incubated for 60 minutes at room temperature with goat anti-rabbit horseradish peroxidase-conjugated IgG (1:3,000; Servicebio, Wuhan, China). After being washed, the labeled proteins were detected with the use of an enhanced chemiluminescence method (ECL kit, Amersham), and the signals were collected on Kodak X-OMAT film (Eastman Kodak, Rochester, NY, USA). The quantity of band intensity was detected and analyzed using Image Quant TL 7.0 analysis software (GE, Pittsburgh, PA, USA).

Immunofluorescence Staining

Rats were deeply anesthetized with the anesthetics mentioned above and perfused with normal saline through the cardiac vascular system, followed by infusion with 4% paraformaldehyde on day 28. The ipsilateral thalamic tissues were harvested, put into the same fixative for 4 hours (4°C), and then cryo-protected in 30% sucrose solution for 48 hours to dehydrate. Several days later, transverse sections (25 μm) were cut on a cryostat. After blocking in 5% normal donkey serum in TBST for 60 minutes at room temperature, the sections were washed with TBST for 10 minutes and incubated overnight in the antibody solution containing rabbit anti-ADCY1 (Solarbio, Beijing, China). The following day, after washing with TBST 3 times for 5-minutes, the sections were incubated for 2 hours with a mixture of corresponding secondary antibody of goat anti-rabbit IgG (1:3,000; Servicebio, Wuhan, China) at room temperature. Fluorescence images were captured by a Nikon Eclipse C1 Ortho microscope (Nikon, Japan).

Statistical Analysis

The statistical software SPSS version 22.0 (SPSS Inc., Chicago, Illinois, USA) was used for processing. All results were expressed as mean ± standard deviation. The differences of multiple samples were analyzed using one-way analysis of variance (ANOVA). Student's t-test was used for comparisons between two groups. $P < 0.05$ was considered to represent a significant difference.

Results

MWTs of the Rats

There was no significant difference in the MWTs value of the bilateral limb and left face at any time point among the 3 groups ($P > 0.05$), as shown in Fig. 2. Results indicated that the MWTs value of the right facial skin in the TP group and EA group decreased significantly on the 3rd day after surgery compared with the SH group ($P < 0.01$). EA began to significantly relieve pain on the 14th day after operation until the end of this trial in the EA group. However, there was no significant change in the TP group. The MWTs values of the rats in the EA group were significantly higher than that of the rats in the TP group ($P < 0.01$) and was close to the MWTs value of the rats in the SH group on the 28th day ($P > 0.05$).

Bioinformatic Analysis

Before analysis, it is important to estimate the quality of the original data in order to ensure the quality of the original sequencing data. The results showed that 36.17 million clean reads per sample were analyzed in

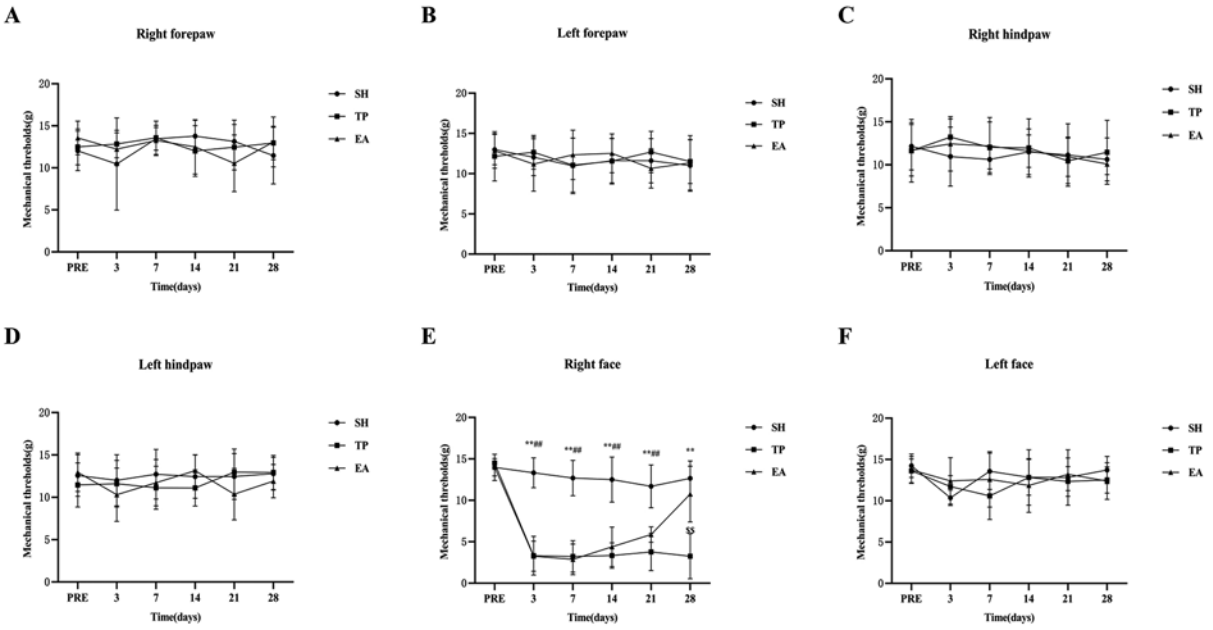

Fig. 2. *Mechanical Withdrawal Thresholds (MWTs). The MWTs of rats were measured at the right forepaw* (A), *left forepaw* (B), *right hind paw* (C), *left hind paw* (D), *right face* (E), *left face* (F) *from presurgery day 3 to the 28th day after operation. MWTs tests were performed 6 times during the experiment. The results showed that there was no significant difference among the 3 groups in the bilateral limb and left face at any time point. As illustrated in* E, *the MWT of the right facial skin in the TP group and the EA group decreased remarkably after operation in comparison to the SH group on postoperative day 3 (**P < 0.01, the TP group vs the SH group; ##P < 0.01, the EA group vs the SH group). From postoperative day 7 to day 28, only the EA treatment group showed improvement in the ipsilateral facial skin (**P < 0.01, the TP group vs the SH group; ##P < 0.01, the EA group vs the SH group; $$P < 0.01, the EA group vs the TP group). n = 6 rats/group.*

the SH group, 36.53 million in the TP group, and 33.34 million in the EA group. The sequencing results are reliable because Q20 of all samples ranged from 96.89% to 98.05%, Q30 from 92.62% to 94.88%, and 89.73% to 92.58% of all samples could map to the reference genome (Table 1).

Differential Gene Expression Profiles among Groups

We performed RNA-seq analysis with 3 samples in each group to investigate the effect of EA on gene expression in the ipsilateral thalamus of TP model rats. The results showed that compared with the SH group, 255 genes were down-regulated in the TP group, and 858 genes were up-regulated. Compared with the TP group, 148 genes were down-regulated in the EA group, and 229 genes were up-regulated (Fig. 3A). The absolute value of log 2 (fold change) ≥ 1.5 or ≤ 0.067 and q-value x < 0.01 were set as filter conditions. To detect the effects of EA treatment on TP, we also screened out the genes that were significantly changed in the TP group compared to the SH group and adjusted back to the baseline by EA stimulation. There were 112 differentially expressed genes (DEGs) that met the above criteria (Fig. 3B). In the volcano map, the DEGs of the TP group vs the SH group and the EA group vs the TP group were shown as in Fig. 3C.

GO Analysis

In order to investigate the potential therapeutic mechanism of EA on TP, we implemented GO enrichment analysis of the DEGs that were up-regulated in the TP group vs SH group and down-regulated in the EA group vs the TP group of rats based on the GO database (Fig. 4). Moreover, we screened out the DEGs that were down-regulated in the TP group vs the sham group and up-regulated in the EA group vs the TP group of rats (Fig. 5). The GO, as an enrichment analysis method, is utilized to annotate the role of genes consisting of biological process (BP), molecular function (MF), and cellular component (CC). In summary, the results of GO analysis indicated that the changes of neural develop-

Table 1. *Quality control and sequencing information for samples.*

Sample	Total clean reads	Total clean bases	Clean reads Q20 (%)	Clean reads Q30 (%)	Total mapping ratio (%)
SH1	36243758	10818618664	97.56	94.02	91.72
SH2	37236488	11099044314	97.81	94.51	92.58
SH3	34924710	10429268102	97.16	92.94	92.04
TP1	36739169	10966824530	98.05	94,88	91.78
TP2	37248213	11135210038	97.64	94.20	92.23
TP3	35613429	10644509336	97.18	93.33	89.73
EA1	34115638	10190957576	97.69	94.29	92.15
EA2	32122792	9590657734	97.12	93.36	90.15
EA3	33776076	9995925692	96.89	92.62	91.03

(1) Sample: sample name, 9 cDNA libraries are SH group (SH1, 2 and 3), TP group (TP1, 2 and 3), EA group (EA1, 2 and 3); (2) Total clean reads: counting the number of total sequencing data after filtering; (3) Total clean bases: the number of total sequencing sequences multiplied by their length; (4) Q20, Q30: counting Phred values, respectively; (5) Total mapping ratio: the ratio of the number of clean reads that can be located on the genome to the number of total clean reads.

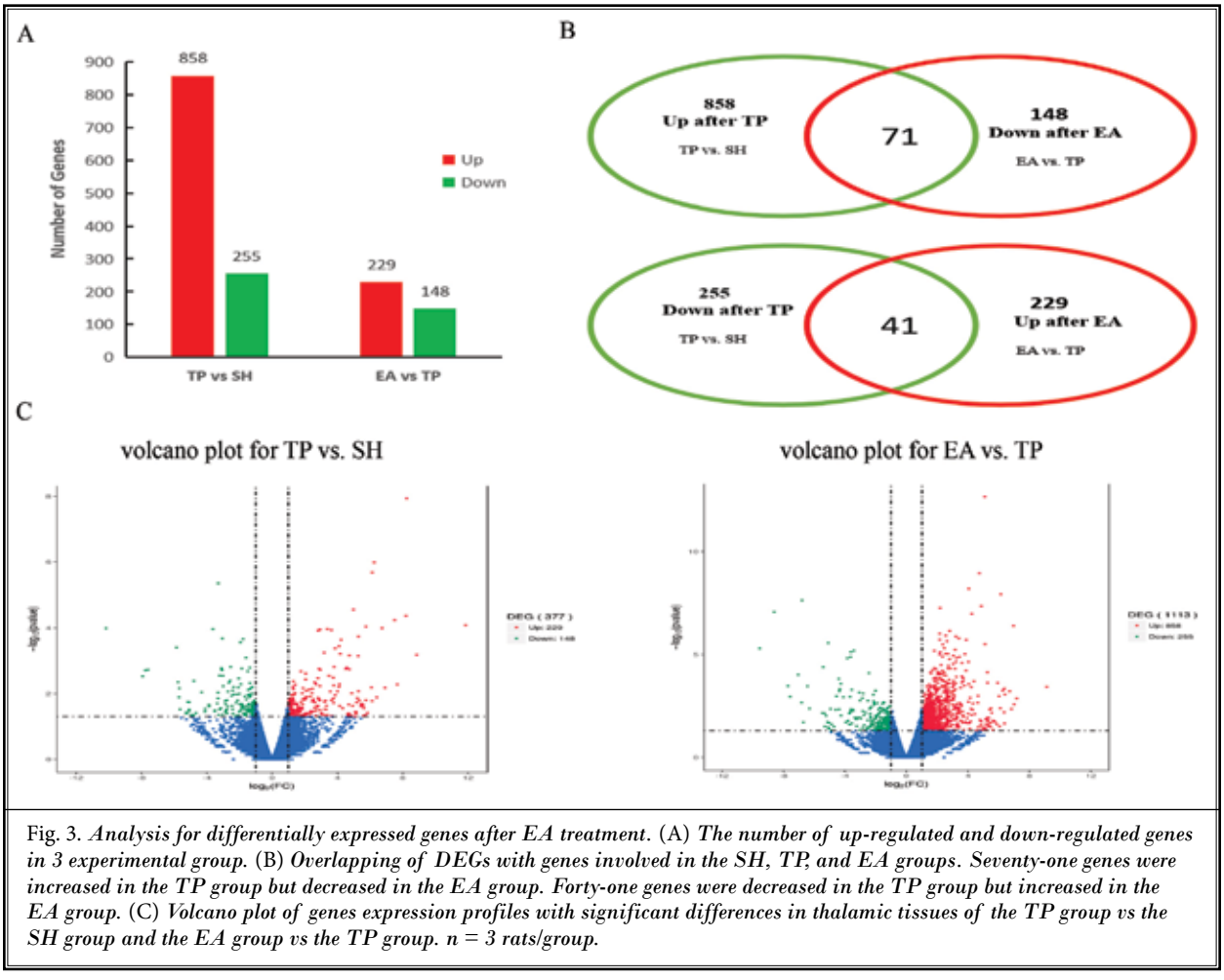

Fig. 3. *Analysis for differentially expressed genes after EA treatment.* (A) *The number of up-regulated and down-regulated genes in 3 experimental group.* (B) *Overlapping of DEGs with genes involved in the SH, TP, and EA groups. Seventy-one genes were increased in the TP group but decreased in the EA group. Forty-one genes were decreased in the TP group but increased in the EA group.* (C) *Volcano plot of genes expression profiles with significant differences in thalamic tissues of the TP group vs the SH group and the EA group vs the TP group. n = 3 rats/group.*

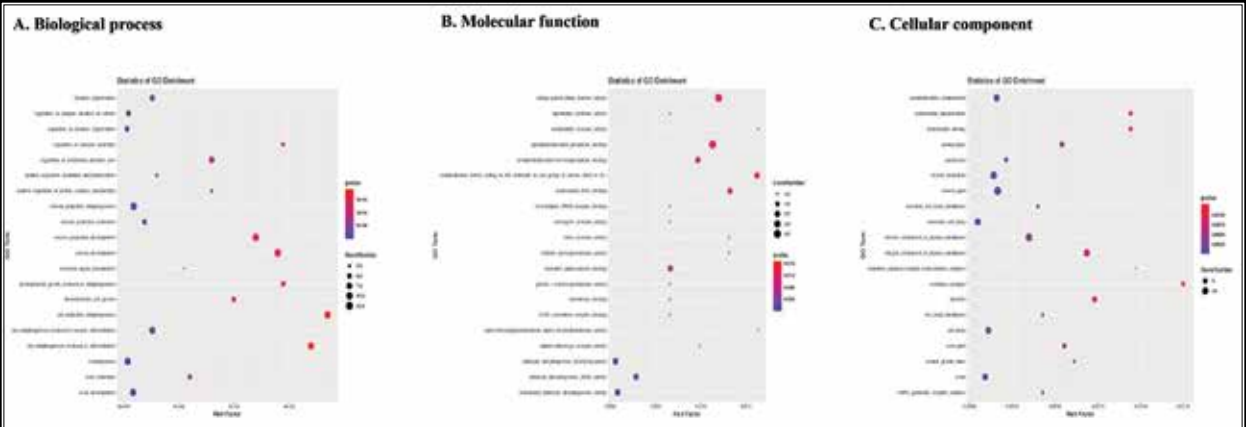

Fig. 4. *Gene Ontology (GO) pathway analysis of Up-regulated DEGs in the TP group vs the SH group and down-regulated DEGs in the EA group vs the TP group.* (A) *Bubble plots showing the top 20 significant biological processes of DEGs.* (B) *Bubble plots showing the top 20 significant molecular functions of DEGs.* (C) *Bubble plots showing the top 20 significant cellular components of DEGs. Larger bubbles indicated higher number of genes. The color of each bubble reflects the significance (P-value).*

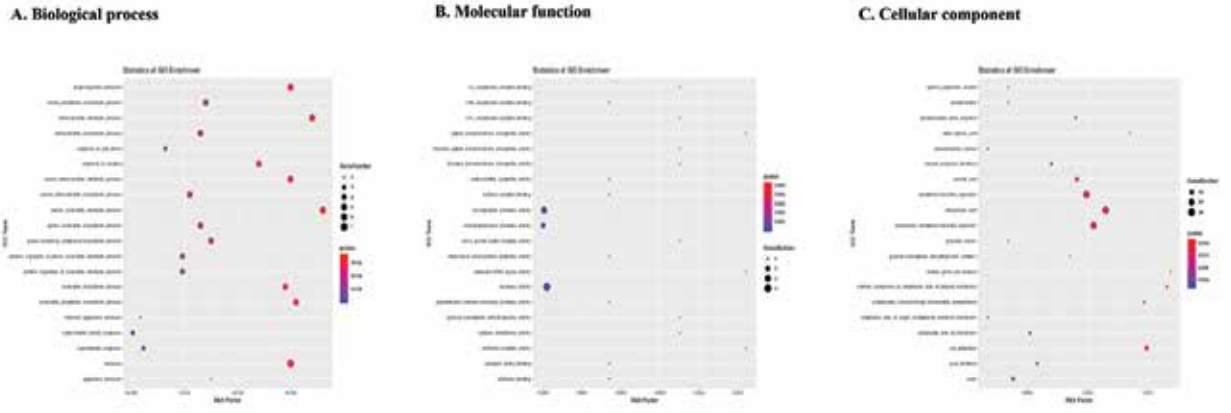

Fig. 5. *Down-regulated DEGs of the TP group vs the SH group and up-regulated DEGs of the EA group vs the TP group.* (A) *Bubble plots showing the top 20 significant biological processes of DEGs.* (B) *Bubble plots showing the top 20 significant molecular functions of DEGs.* (C) *Bubble plots showing the top 20 significant cellular components of DEGs. Larger bubbles indicated higher number of genes. The color of each bubble reflects the significance (P-value).*

ment and signal transduction pathway were closely related to TP and the therapeutic effect of EA.

Analysis of Important KEGG Pathways

KEGG pathway analysis was performed to further analyze the DEGs among the 3 experimental groups. Pathway classification statistics showed that the up-regulated DEGs in the TP group vs the SH group and down-regulated DEGs in the EA group vs the TP group were exclusively involved in 83 pathways, which included "Oxytocin signaling pathway," "cAMP signaling pathway," "GABAergic synapse," etc. (Fig. 6A). KEGG analysis also indicated that the down-regulated DEGs in the TP group vs the SH group and up-regulated DEGs in the EA group vs the TP group were significantly enriched in 49 pathways, which included "Thiamine metabolism", "Sulfur relay system," "Neuroactive ligand-receptor interaction," etc. (Fig. 6B).

RNA-Seq Data Validation Using PCR

Next, PCR was used to test the reliability of RNA-Seq data in this study. We evaluated the DEGs which

were implicated in the ion channel of pain signal transduction identified by GO analysis. We found that the expression of ADCY1 genes was significantly up-regulated in the TP group, subsequently down-regulated by EA treatment (Fig. 7A). The tendency was found to be identical to the results obtained by RNA-Seq, as shown in Fig. 7B. As a consequence, the RNA-Seq data was reliable for gene expression profile analysis according to the PCR results.

Western Blotting Detection Results

As shown in Fig. 8, the data demonstrated that the rats of the TP group showed significantly high levels of ADCY1 protein than the rats of the sham group, indi-

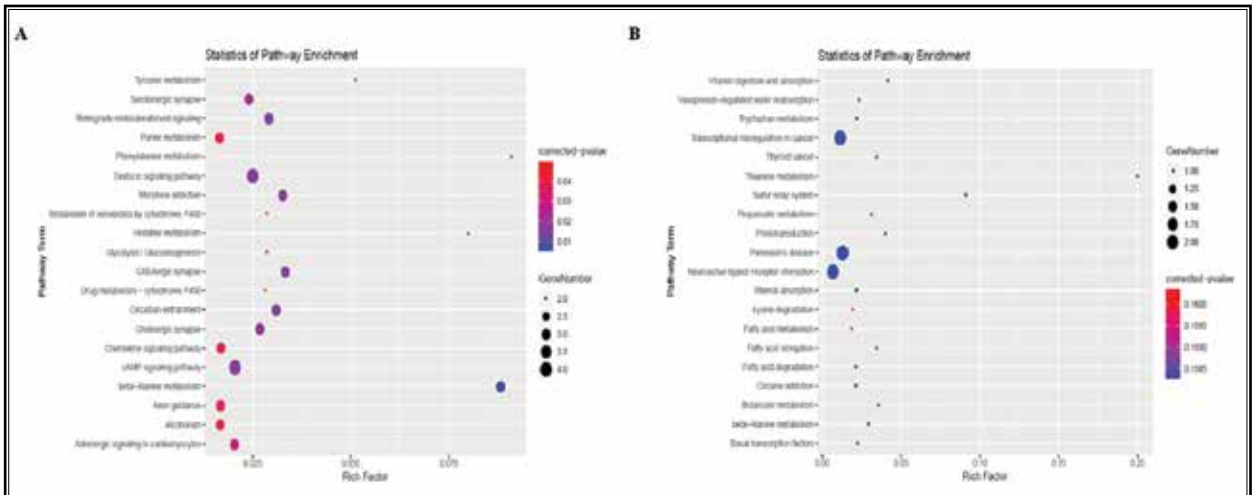

Fig. 6. (A) *KEGG pathway analysis of up-regulated DEGs in the TP group vs the SH group and down-regulated DEGs in the EA group vs the TP group. Bubble plots showing the top 20 significant pathways of DEGs. Larger bubbles indicated higher number of genes. The color of each bubble reflects the significance (P-value).* (B) *KEGG pathway analysis of down-regulated DEGs in the TP group vs the SH group and up-regulated DEGs in the EA group vs the TP group. Bubble plots showing the top 20 significant pathways of DEGs. Larger bubbles indicated higher number of genes. The color of each bubble reflects the significance (P-value).*

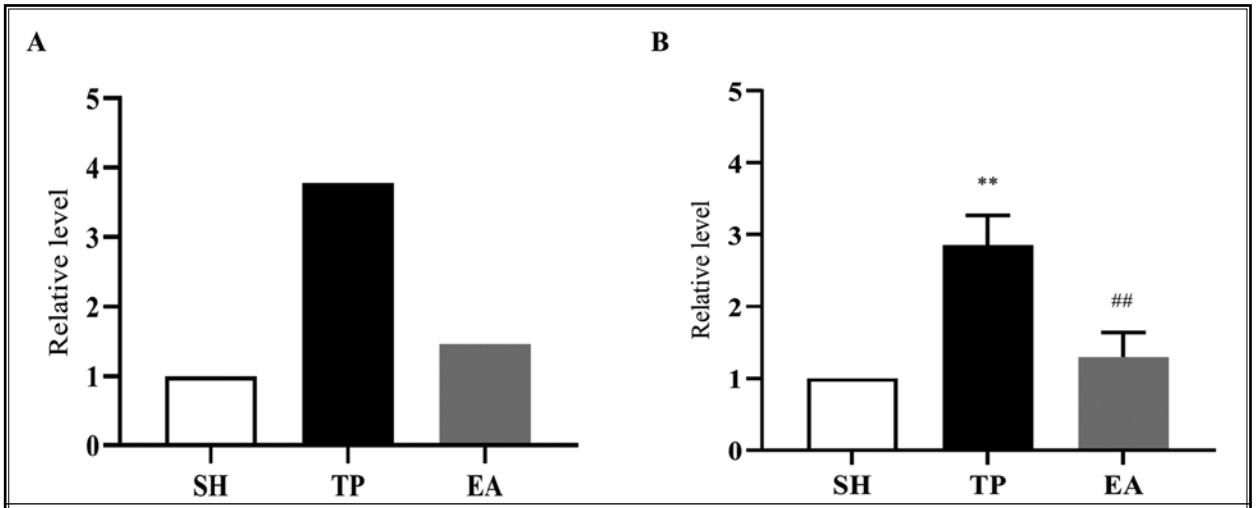

Fig. 7. *The validation of RNA-Seq results using PCR.* (A) *The expression of ADCY1 genes by RNA-Seq.* (B)*The expression of ADCY1 genes in immune response was detected by PCR. **$P < 0.01$, compared with the SH group. ##$P < 0.01$, compared with the TP group. $n = 3$ rats/group.*

cating higher levels in the thalamic tissues during TP. Repeated EA treatment significantly reduced ADCY1 protein overexpression of TP rats. These results suggested that the up-regulation of ADCY1 expression in the thalamic tissues of TP rats may be associated with TP, and the therapeutic effect of EA on TP may be related to ADCY1.

Immunofluorescence Staining Detection Results

To evaluate the role of ADCY1 in EA treatment in TP rats, the levels of ADCY1 protein expression were detected on day 28 post-surgery. After immunofluorescence staining, the expression of ADCY1 protein in the thalamic tissues was observed. In comparison with the SH group, AC1 protein expression in the TP group was markedly increased ($P < 0.01$). However, the expression intensity of ADCY1 protein in the EA group was significantly lower than that in the TP group ($P < 0.01$) (Fig. 9).

Discussion

Pharmacotherapy is currently the first-line treatment of TP according to the International Association for the Study of Pain (IASP) (13). Despite this, all approved drugs have limited efficacy and are associated with troubling side effects (14-16). Neuromodulation has emerged as a specific form of pain treatment in addition to these pharmacotherapies (17). These neuro-

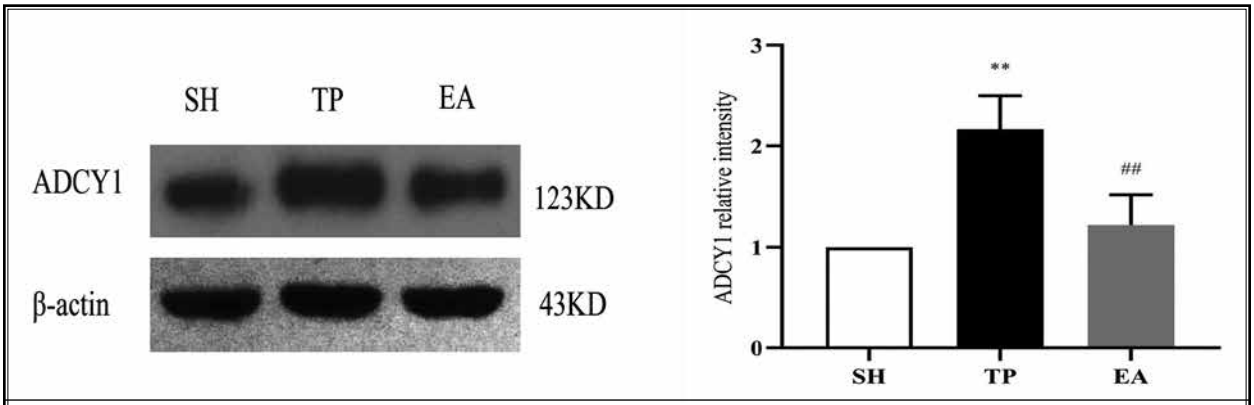

Fig. 8. *EA attenuates the upregulation of ADCY1 protein expression in thalamic tissues of CV-treated TP rats. The determination of ADCY1 protein expression by Western blot. Typical bands and averaged data showed that ADCY1 protein was upregulated in TP rats, and EA attenuated upregulation of ADCY1 protein. **P < 0.01 the TP group vs the SH group. ##P < 0.01 the EA group vs the TP group. n = 3 rats/group.*

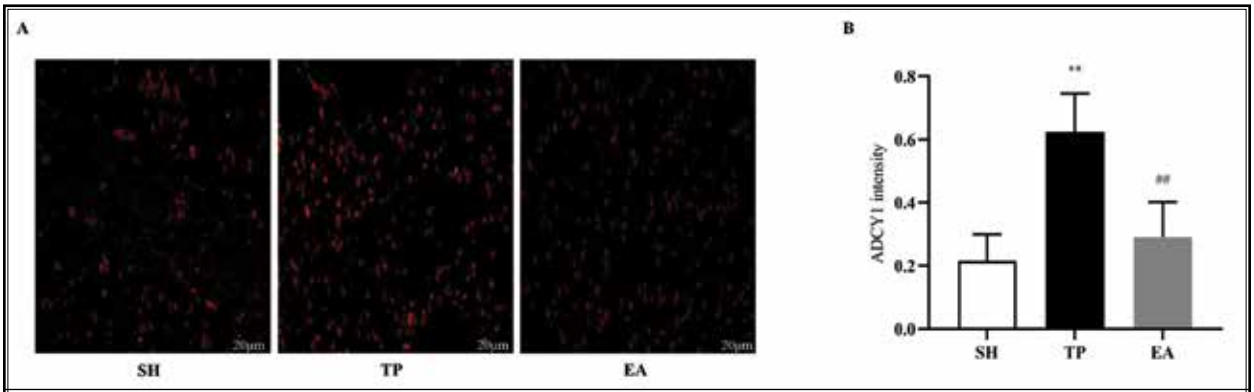

Fig. 9. *Effect of EA on the expression of the ADCY1 protein in thalamic tissues of each group shown by using immunofluorescence. The tissues of the thalamus were harvested on day 28 after operation.* (A) *Immunostaining shows the expression of the ADCY1 protein in the SH, TP, and EA groups, respectively.* (B) *Summarized intensity of the ADCY1 protein in each observation field from the SH, TP, and EA groups. **P < 0.01 the TP group vs SH group. ##P < 0.01 the EA group vs. TP group. n = 3 rats/group.*

modulatory therapies include motor cortex stimulation (MCS), deep brain stimulation (DBS), non-invasive treatments of repetitive transcranial magnetic stimulation (rTMS), transcranial direct current stimulation (tDCS), and transcutaneous electrical nerve stimulation (TENS) (18). These modalities have also been implemented to treat TP syndromes (19-23).

Both therapeutic effectiveness and similar neurochemical mechanisms may be involved in processing EA and TENS analgesia (24). The efficacy of EA in TP control and well-being are in agreement with prior studies (25). In a study of the recovery outcomes in stroke survivors with shoulder pain, EA was felt to be effective in reducing shoulder pain and improving upper extremity function (26). There is also a report that TP can be relieved by EA treatment by inhibiting autophagy in the rat hippocampus (27). These results are quite similar to our previous outcomes. We established a new TP rat model produced by administration of cobra venom into the left VPL nucleus and confirmed that EA treatment can ameliorate neuropathic pain and restore the ultrastructural alterations of the damaged regions of the brain (11). Although many different studies had shown that EA has analgesic effects in treating TP, the molecular mechanism of EA analgesia remains an open question. Therefore, based on our previous work, we further explored the basis for its molecular mechanism. The present study shows that the mechanical pain thresholds were significantly improved after EA stimulation, suggesting a satisfactory analgesic effect of EA treatment in TP rats. We have successfully identified that many DEGs were significantly raised or lowered in association with EA therapy. We found that 3 significant pathways, including oxytocin signaling pathway, cyclic adenosine 3, 5'-monophosphate (cAMP) signaling pathway, and GABAergic synapse were affected in the TP rat model by EA treatment via transcriptomic analysis. In addition, ADCY1 was closely related to the above 3 pathways. The expression of ADCY1 in the TP group was significantly higher than that in SH group, while it declined very close to the level seen in the SH group after EA intervention. The results of PCR revealed similar changes to the gene expression analyses. Both western blot and immunofluorescence detection supported our findings in the changes of ADCY1 protein among the 3 groups.

ADCY1, a main downstream signal protein of N-methyl-D-aspartate (NMDA) receptor, is a potential novel target for treating chronic pain and has been widely studied (28,29). ADCY1 significantly promotes behavioral sensitization and spinal facilitation in pain models in animals (30). ADCY1 may induce both presynaptic and postsynaptic forms of long-term potentiation (LTP). The trigger of LTP is closely related to the transmission, relay, and perception of pain. According to the retrospective data to date, ADCY1 is the primary target for the treatment of chronic pain, including neuropathic and inflammatory pain (31). Ding et al found that ADCY1 was associated with alcohol-induced inflammatory pain and exercise sensitization. Heterosensitization of ADCY1 is caused by the enhancement of the cAMP response (32). Therefore, ADCY1 has become a promising new focus of targeted therapeutics for opioid abuse in chronic pain (33). In a rat model of tooth-related injury, inhibitors of ADCY1 (ST034307) significantly decreased the grimace scale and mouth wiping scores, accompanied by reductions in cAMP generation, protein kinase A (PKA) activation, and NMDA receptor expression in the anterior cingulate cortex (34). Painful diabetic neuropathy (PDN) is characterized by severe neuropathic pain, which can be attenuated with the intrathecal administration of an inhibitor of ADCY1 (NB001) (35). The repetitive EA pretreatment can inhibit the function of ADCY1, PKA, and the L-type Ca2+ channel (36).

The present study also had limitations. Firstly, our selected screening method for candidate genes may narrow the range so that other key genes were missed. Secondly, we only detected the change of ADCY1 protein expression but did not detect its upstream/downstream signal pathway, so we didn't know whether the expressions of other related proteins had also changed. Thirdly, our current results only provided preliminary evidence for the molecular mechanism of EA in the treatment of TP. Gene knockout technology should be developed and examined to provide more convincing results.

Conclusions

Our results show that EA can reduce the pain response in a rat model of TP and is associated with the downregulation of multiple genes including ADCY1, which may be a key element. Thus, our work provides a theoretical support for clinical massage and EA treatment of TP symptoms and may initiate a scientific basis for alternative therapeutic strategies in the management of central neuropathic pain.

Author's Participation

Bao-Feng Ma- Ideas; Formulation or evolution of

overarching research goals and aims; Development or design of methodology; Creation of models; Writing the initial draft.

Jian-Feng Zhang- Data collection and curation; Statistical, mathematical, and computational application to analyze or synthesize study data; Preparation, creation, and presentation of the publishing work.

John P. Williams- Writing - Review & Editing; Preparation, creation, and presentation of the publishing work.

Ruo-Guo Wang- Creation of models; Provision of study materials, animals, reagents, laboratory samples, instrument.

Jian Guo- Creation of models; Data collection and curation.

Jian-Xiong An- Funding acquisition; Management and coordination responsibility; Oversight and leadership responsibility; Ensuring that the descriptions are accurate and agreed by all authors.

References

1. Cai Q, Guo Q, Li Z, et al. Minimally invasive evacuation of spontaneous supratentorial intracerebral hemorrhage by transcranial neuroendoscopic approach. *Neuropsychiatr Dis Treat* 2019; 15:919-925.
2. Guédon A, Thiebaut JB, Benichi S, Mikol J, Moxham B, Plaisant O. Dejerine-Roussy syndrome: Historical cases. *Neurology* 2019; 93:624-629.
3. Lo Buono V, Corallo F, Bramanti P, Marino S. Coping strategies and health-related quality of life after stroke. *J Health Psychol* 2017; 22:16-28.
4. Klit H, Finnerup NB, Jensen TS. Central post-stroke pain: clinical characteristics, pathophysiology, and management. *Lancet Neurol* 2009; 8:857-868.
5. Kumar B, Kalita J, Kumar G, Misra UK. Central poststroke pain: a review of pathophysiology and treatment. *Anesth Analg* 2009; 108:1645-1657.
6. Finnerup NB, Kuner R, Jensen TS. Neuropathic pain: from mechanisms to treatment. *Physiol Rev* 2021; 101:259-301.
7. Zhao ZQ. Neural mechanism underlying acupuncture analgesia. *Prog Neurobiol* 2008; 85:355-375.
8. Ali U, Apryani E, Wu HY, Mao XF, Liu H, Wang YX. Low frequency electroacupuncture alleviates neuropathic pain by activation of spinal microglial IL-10/β-endorphin pathway. *Biomed Pharmacother* 2020; 125:109898.
9. Cong W, Peng Y, Meng B, Jia X, Jin Z. The effect of electroacupuncture on regulating pain and depression-like behaviors induced by chronic neuropathic pain. *Ann Palliat Med* 2021; 10:104-113.
10. Li Y, Yin C, Li X, et al. Electroacupuncture alleviates paclitaxel-induced peripheral neuropathic pain in rats via suppressing TLR4 signaling and TRPV1 upregulation in sensory neurons. *Int J Mol Sci* 2019; 20:5917.
11. An JX, Shi WR, Zhang JF, et al. A new rat model of thalamic pain produced by administration of cobra venom to the unilateral ventral posterolateral nucleus. *Pain Physician* 2019; 22:E635-e647.
12. Chaplan SR, Bach FW, Pogrel JW, Chung JM, Yaksh TL. Quantitative assessment of tactile allodynia in the rat paw. *J Neurosci Methods* 1994; 53:55-63.
13. Urits I, Gress K, Charipova K, et al. Diagnosis, treatment, and management of Dejerine-Roussy syndrome: a comprehensive review. *Curr Pain Headache Rep* 2020; 24:48.
14. Wan L, Li Z, Liu T, et al. Epoxyeicosatrienoic acids: emerging therapeutic agents for central post-stroke pain. *Pharmacol Res* 2020; 159:104923.
15. Yang F, Fu H, Lu YF, et al. Post-stroke pain hypersensitivity induced by experimental thalamic hemorrhage in rats is region-specific and demonstrates limited efficacy of gabapentin. *Neurosci Bull* 2014; 30:887-902.
16. Kim JS, Bashford G, Murphy KT, Martin A, Dror V, Cheung R. Safety and efficacy of pregabalin in patients with central post-stroke pain. *Pain* 2011; 152:1018-1023.
17. Wang J, Chen Z. Neuromodulation for pain management. *Adv Exp Med Biol* 2019; 1101:207-223.
18. Knotkova H, Hamani C, Sivanesan E, et al. Neuromodulation for chronic pain. *Lancet* 2021; 397:2111-2124.
19. Watson JC, Sandroni P. Central neuropathic pain syndromes. *Mayo Clin Proc* 2016; 91:372-385.
20. Hosomi K, Seymour B, Saitoh Y. Modulating the pain network--neurostimulation for central poststroke pain. *Nat Rev Neurol* 2015; 11:290-299.
21. Pickering AE, Thornton SR, Love-Jones SJ, Steeds C, Patel NK. Analgesia in conjunction with normalisation of thermal sensation following deep brain stimulation for central post-stroke pain. *Pain* 2009; 147:299-304.
22. Hasan M, Whiteley J, Bresnahan R, et al. Somatosensory change and pain relief induced by repetitive transcranial magnetic stimulation in patients with central poststroke pain. *Neuromodulation* 2014; 17:731-736.
23. Kadono Y, Koguchi K, Okada KI, et al. Repetitive transcranial magnetic stimulation restores altered functional connectivity of central poststroke pain model monkeys. *Sci Rep* 2021; 11:6126.
24. Wang JQ, Mao L, Han JS. Comparison of the antinociceptive effects induced by electroacupuncture and transcutaneous electrical nerve stimulation in the rat. *Int J Neurosci* 1992; 65:117-129.
25. Santos AB, Gozzani JL. Acupuncture as adjuvant therapy in thalamic syndrome: case report. *Rev Bras Anestesiol* 2011; 61:88-94.
26. Chau JPC, Lo SHS, Yu X, et al. Effects of acupuncture on the recovery outcomes of stroke survivors with shoulder pain: a systematic review. *Front Neurol* 2018; 9:30.
27. Zheng L, Li XY, Huang FZ, et al. Effect of electroacupuncture on relieving central post-stroke pain by inhibiting autophagy in the hippocampus. *Brain Res* 2020; 1733:146680.
28. Kreutzwiser D, Tawfic QA. Expanding role of NMDA receptor antagonists in the management of pain. *CNS Drugs* 2019; 33:347-374.
29. Li XH, Chen QY, Zhuo M. Neuronal adenylyl cyclase targeting central plasticity for the treatment of chronic pain. *Neurotherapeutics* 2020; 17:861-873.
30. Wang H, Xu H, Wu LJ, et al. Identification of an adenylyl cyclase inhibitor for

treating neuropathic and inflammatory pain. *Sci Transl Med* 2011; 3:65ra3.

31. Zhuo M. Targeting neuronal adenylyl cyclase for the treatment of chronic pain. *Drug Discov Today* 2012; 17:573-582.
32. Ding Z, Knipp GT, van Rijn RM, Chester JA, Watts VJ. The CUL3/neddylation inhibitor MLN4924 reduces ethanol-induced locomotor sensitization and inflammatory pain allodynia in mice. *Behav Brain Res* 2021; 399:113051.
33. Kaur J, Soto-Velasquez M, Ding Z, et al. Optimization of a 1,3,4-oxadiazole series for inhibition of Ca(2+)/calmodulin-stimulated activity of adenylyl cyclases 1 and 8 for the treatment of chronic pain. *Eur J Med Chem* 2019; 162:568-585.
34. Cheng Y, Huang P, Meng B, Gan L, Wu D, Cao Y. Antinociceptive effects of the adenylyl cyclase inhibitor ST034307 on tooth-movement-induced nociception in rats. *Arch Oral Biol* 2019; 98:81-86.
35. Griggs RB, Santos DF, Laird DE, et al. Methylglyoxal and a spinal TRPA1-AC1-Epac cascade facilitate pain in the db/db mouse model of type 2 diabetes. *Neurobiol Dis* 2019; 127:76-86.
36. Gao J, Zhang L, Wang Y, et al. Antiarrhythmic effect of acupuncture pretreatment in rats subjected to simulative global ischemia and reperfusion--involvement of adenylate cyclase, protein kinase A, and L-type Ca2+ channel. *J Physiol Sci* 2008; 58:389-396.